A New 4-D Hyperchaotic Two-Wing System with a Unique Saddle-Point Equilibrium at the Origin, its Bifurcation Analysis and Circuit Simulation

S. Vaidyanathan[1,*], I. M. Moroz[2], A. Sambas[3], Mujiarto[3] and W. S. M. Sanjaya[4]

[1] Research and Development Centre, Vel Tech University, Avadi, Chennai, India
[2] Mathematical Institute, University of Oxford, Andrew Wiles Building, ROQ, Oxford Ox2 6GG, UK
[3] Department of Mechanical Engineering, Universitas Muhammadiyah Tasikmalaya, Indonesia
[4] Department of Physics, Universitas Islam Negeri Sunan Gunung Djati, Bandung, Indonesia

[*]sundarvtu@gmail.com

Abstract. A new 4-D hyperchaotic two-wing system with three quadratic nonlinearities is proposed in this paper. The dynamical properties of the new hyperchaotic system are described in terms of phase portraits, Lyapunov exponents, Kaplan-Yorke dimension, symmetry, dissipativity, etc. Also, a detailed dynamical bifurcation analysis of the hyperchaotic system has been studied using bifurcation diagrams. As an engineering application, an electronic circuit realization of the new hyperchaotic two-wing system is developed in MultiSIM, which confirms the feasibility of the theoretical hyperchaotic two-wing system.

1. Introduction

Chaos theory deals with nonlinear dynamical systems exhibiting high sensitivity to small changes in initial conditions [1-2]. Mathematically, chaotic systems are characterized by the presence of at least one positive Lyapunov exponent. Chaotic systems are very useful in many applications in science and engineering such as weather systems [3-5], ecology [6-10], neurons [11-12], biology [13-16], cellular neural networks [17-18], chemical reactors [19-24], brain waves [25-26], Tokamak systems [27-28], oscillators [29-35], encryption [36-44], finance systems [45-46], circuits [47-50], etc.

Hyperchaotic systems are defined as nonlinear dynamical systems having two or more positive Lyapunov exponents [1-2]. They exhibit more complex behaviour than chaotic dynamical systems as the trajectories of hyperchaotic systems can expand in two different directions corresponding to the two positive Lyapunov exponents.

Many new hyperchaotic systems with special behaviour have been reported in the literature such as hyperchaotic Lorenz system [51], hyperchaotic Chen system [52], hyperchaotic Lü system [53], hyperchaotic Vaidyanathan systems [54-55], etc.

In this research paper, a new 4-D hyperchaotic two-wing system with three quadratic nonlinearities is proposed and the dynamical properties of the new hyperchaotic system are described in terms of phase portraits, Lyapunov exponents, Kaplan-Yorke dimension, symmetry, dissipativity, etc. Also, a

detailed dynamical bifurcation analysis of the hyperchaotic system has been studied using bifurcation diagrams. As an engineering application, an electronic circuit realization of the new hyperchaotic two-wing system is developed in MultiSim, which confirms the feasibility of the theoretical hyperchaotic two-wing system.

Section 2 describes the new hyperchaotic two-wing system, its phase plots and Lyapunov exponents. Section 3 describes the dynamic analysis of the new hyperchaotic two-wing system. Furthermore, an electronic circuit realization of the new chaotic system is presented in detail in Section 4. The circuit experimental results of the new hyperchaotic system in Section 4 show good agreement with the numerical simulations via MATLAB obtained in Section 2. Section 5 draws the main conclusions of this research work.

2. A New Hyperchaotic Two-Wing system with Three Quadratic Nonlinearities

In this work, we report a new 4-D dynamical system given by

$$\begin{cases} \dot{x} = a(y-x) + yz + w \\ \dot{y} = by - xz + w \\ \dot{z} = -cz + xy \\ \dot{w} = -dx \end{cases} \tag{1}$$

where $X = (x, y, z, w)$ is the state and a, b, c, d are positive constants.

In this paper, we show that the 4-D system (1) is *hyperchaotic* for the parameter values

$$a = 33,\ b = 18,\ c = 5,\ d = 4 \tag{2}$$

Using Wolf's algorithm [56], the Lyapunov exponents of the system (1) for the parameter set $(a, b, c, d) = (33, 18, 5, 4)$ and the initial state $X(0) = (0.1, 0.2, 0.1, 0.2)$ were found as

$$LE_1 = 2.3201,\ LE_2 = 0.0307,\ LE_3 = 0,\ LE_4 = -22.3468 \tag{3}$$

Thus, the 4-D system (1) is hyperchaotic with two positive Lyapunov exponents.

It is noted that the sum of the Lyapunov exponents in (3) is negative.

$$LE_1 + LE_2 + LE_3 + LE_4 = -22 < 0 \tag{4}$$

This shows that the system (1) is dissipative with a strange hyperchaotic attractor.

The Kaplan-Yorke dimension of the system (1) is computed as

$$D_{KY} = 3 + \frac{LE_1 + LE_2 + LE_3}{|LE_4|} = 3.1052 \tag{5}$$

Figure 1 shows the Lyapunov exponents of the 4-D dissipative hyperchaotic system (1) for the parameter set $(a, b, c, d) = (33, 18, 5, 4)$ and initial state $X(0) = (0.1, 0.2, 0.1, 0.2)$.

We observe that the 4-D hyperchaotic system (1) remains invariant under the change of coordinates given by

$$(x, y, z, w) \mapsto (-x, -y, z, -w) \tag{6}$$

This shows that the 4-D hyperchaotic system (1) has rotation symmetry about the $z-$axis for all values of the parameters $a, b, c,$ and d. Hence, any non-trivial trajectory $(x(t), y(t), z(t), w(t))$ of the system (1) must also have a twin trajectory $(-x(t), -y(t), z(t), -w(t))$ of the same system (1).

Figures 2-5 show the 2-D phase portraits of the hyperchaotic system (1) for the parameter set $(a, b, c, d) = (33, 18, 5, 4)$ and initial state $X(0) = (0.1, 0.2, 0.1, 0.2)$. from the phase plots, we see that the 4-D system (1) has a *hyperchaotic two-wing attractor*.

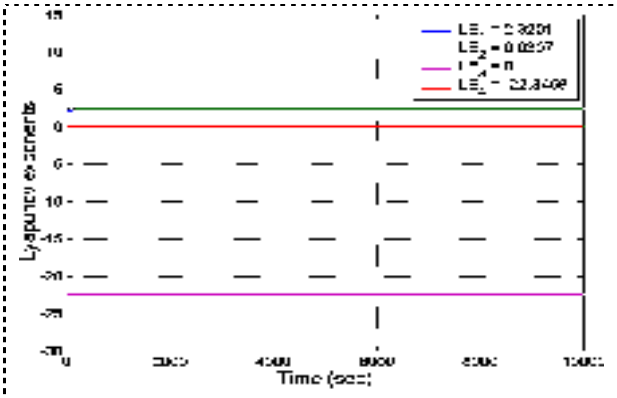

Figure 1. Lyapunov exponents of the hyperchaotic two-wing system (1) for the parameter set $(a,b,c,d)=(33,18,5,4)$ and initial state $X(0)=(0.1,0.2,0.1,0.2)$

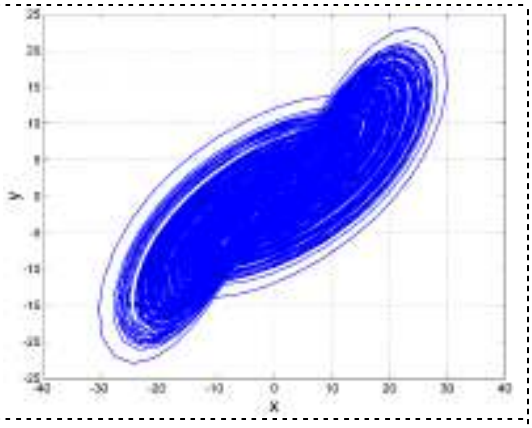

Figure 2. MATLAB plot showing the 2-D phase portrait of the hyperchaotic two-wing system (1) in the $(x,y)-$plane for $(a,b,c,d)=(33,18,5,4)$ and $X(0)=(0.1,0.2,0.1,0.2)$

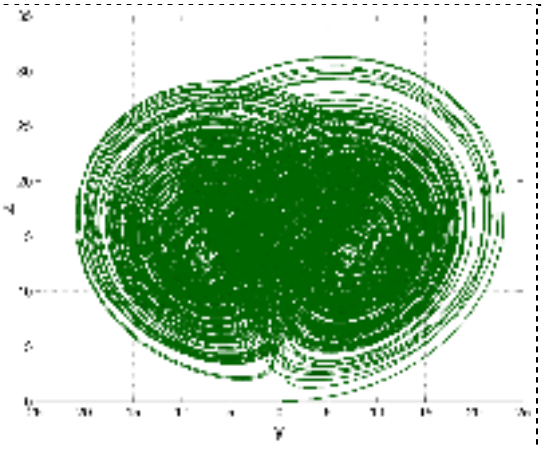

Figure 3. MATLAB plot showing the 2-D phase portrait of the hyperchaotic two-wing system (1) in the $(x,z)-$plane for $(a,b,c,d)=(33,18,5,4)$ and $X(0)=(0.1,0.2,0.1,0.2)$

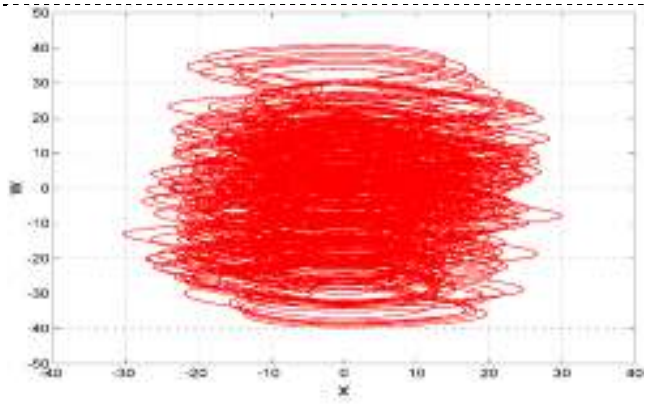

Figure 4. MATLAB plot showing the 2-D phase portrait of the hyperchaotic two-wing system (1) in the $(x,w)-$plane for $(a,b,c,d)=(33,18,5,4)$ and $X(0)=(0.1,0.2,0.1,0.2)$

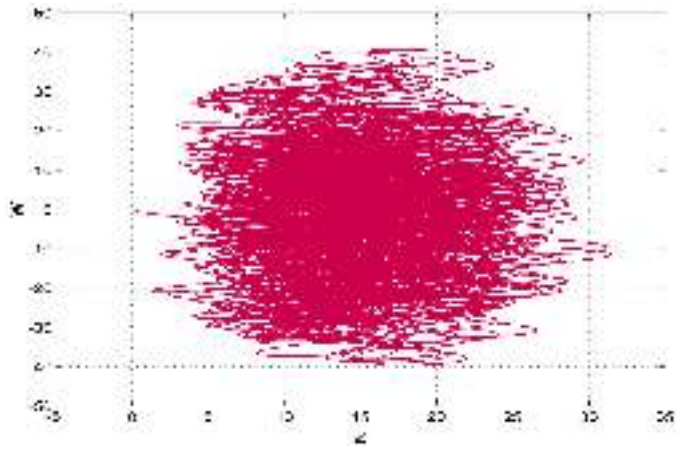

Figure 5. MATLAB plot showing the 2-D phase portrait of the hyperchaotic two-wing system (1) in the $(z,w)-$plane for $(a,b,c,d)=(33,18,5,4)$ and $X(0)=(0.1,0.2,0.1,0.2)$

The equilibrium points of the new hyperchaotic system (1) are obtained by solving the system

$$a(y-x)+yz+w=0 \tag{7a}$$
$$by-xz+w=0 \tag{7b}$$
$$-cz+xy=0 \tag{7c}$$
$$-dx=0 \tag{7d}$$

From (7d), we deduce that $x=0.$ Substituting $x=0$ in (7c), we get $z=0.$

Substituting $x=z=0$ in (7a) and (7b), we get

$$ay+w=0 \text{ and } by+w=0 \tag{8}$$

Solving (8), we get $(a-b)y=0.$ Since $a\neq b$ for the hyperchaotic case (2), we must have $y=0.$

Substituting $y=0$ in (8), we get $w=0.$

Hence, $E_0=(0,0,0,0)$ is the only equilibrium point of the 4-D hyperchaotic system (1).

The Jacobian matrix of the new hyperchaotic system (1) at $E_0=(0,0,0,0)$ is obtained as

$$J=\begin{bmatrix}-a & a & 0 & 1\\ 0 & b & 0 & 1\\ 0 & 0 & -c & 0\\ -d & 0 & 0 & 0\end{bmatrix}=\begin{bmatrix}-33 & 33 & 0 & 1\\ 0 & 18 & 0 & 1\\ 0 & 0 & -5 & 0\\ -4 & 0 & 0 & 0\end{bmatrix} \tag{9}$$

The Jacobian matrix J has the spectral values $-5,-32.9572,0.1020$ and $17.8553.$

This shows that the equilibrium point E_0 is a saddle point and unstable.

Hence, we conclude that the 4-D hyperchaotic system (1) has self-excited attractor [2].

3. Dynamic Analysis for the New Hyperchaotic System

3.1 Equilibrium points for the new hyperchaotic system

The four-dimensional hyperchaotic system introduced in this work is given by

$$\begin{aligned}\dot{x} &= a(y-x)+yz+w = F(x,y,z,w)\\ \dot{y} &= by-xz+w = G(x,y,z,w)\\ \dot{z} &= -cz+xy = H(x,y,z,w)\\ \dot{w} &= -dx = K(x,y,z,w)\end{aligned} \tag{10}$$

The divergence of the flow defined by the system (10) is

$$\frac{\partial F}{\partial x}+\frac{\partial G}{\partial y}+\frac{\partial H}{\partial z}+\frac{\partial K}{\partial w} = -(a+c-b), \tag{11}$$

which is negative for the chosen parameter values (2). Thus, the trajectories of the 4-D system (10) evolve to lie within a bounded region of the phase space.

In Section 2, we showed that the trivial fixed point $E_0 = (0,0,0,0)$ is the only equilibrium point of the new hyperchaotic system (10).

Linear stability of the equilibrium state E_0 is found by computing the fourth order Jacobian matrix J_e evaluated at the equilibrium state:

$$J_e = \begin{bmatrix} -a & a & 0 & 1 \\ 0 & b & 0 & 1 \\ 0 & 0 & -c & 0 \\ -d & 0 & 0 & 0 \end{bmatrix} \tag{12}$$

Linear stability is found by analyzing the characteristic polynomial of J_e, which is the determinant of $J_e - \lambda I_4$, where λ give the eigenvalues and I_4 is the $(4,4)$ identity matrix. One factor of $\varphi(\lambda) = \det(J_e - \lambda I_4)$ is $(\lambda + c)$, leaving a cubic polynomial for the three remaining eigenvalues:

$$\lambda^3 + (a-b)\lambda^2 + (d-ab)\lambda + d(a-b) = 0 \tag{13}$$

3.2 Bifurcations

A steady bifurcation occurs when $\lambda = 0,$ which implies that $d = 0$ or $a = b.$ Neither possibility is allowed here, because of the assumptions that all four parameters are positive, with $a \neq b.$

We now consider the possibility of a simple Hopf bifurcation. Substituting $\lambda = iw$ into (13) gives two equations for w^2, *viz.* either $w^2 = d$ or $w^2 = d - ab,$ which cannot be both satisfied unless a or b vanish.

3.3 Numerical Integrations

In our numerical integrations, we vary each parameter in turn to create a series of bifurcation transition diagrams in terms of $x_{\max}.$ Figure 6 shows a bifurcation transition plot of $x_{\max}$ as a decreases. The dynamics is predominantly chaotic for $a > 25.3,$ with a window of period-3 orbits and their period-doubling bifurcations for $30.98 < a < 31.17$ (see Figure 7). $a = 33$ falls within the second of the chaotic regions.

Figure 8 shows the bifurcation transition plot of the maxima of x over each cycle as b increases. There is a period-3 window for $19.34 < b < 19.47,$ while the parameter choice of $b = 18$ falls within the initial chaotic regime.

Next, we show the bifurcation transition plot of $x_{\max}$ as c decreases from $c=15$ to $c=0$. We note that $c=5$ clearly falls within the first chaotic regime (see Figure 9), and there is a reverse period-doubling cascade for the period-3 orbit in $7.32<c<8.24$.

Finally, Figure 10 shows the bifurcation transition plot for $x_{\max}$ as d increases. Clearly visible is the reverse period-doubling bifurcation for the period-3 cycle in $10.48<d<12.2$. The parameter choice of $d=4$ falls well within the first chaotic region.

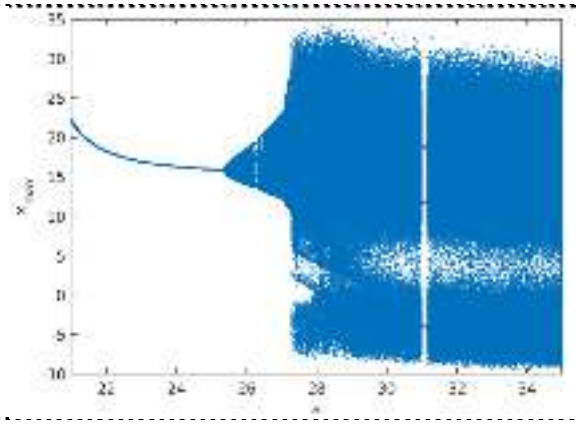

Figure 6. Part of the bifurcation transition plot of $x_{\max}$ as a decreases for the 4-D system (10)

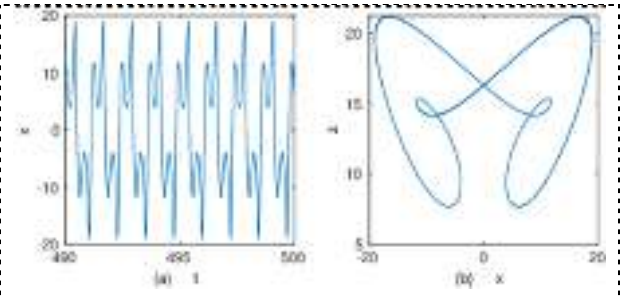

Figure 7. An example of a period-3 orbit of the 4-D system (10) for $a=31$

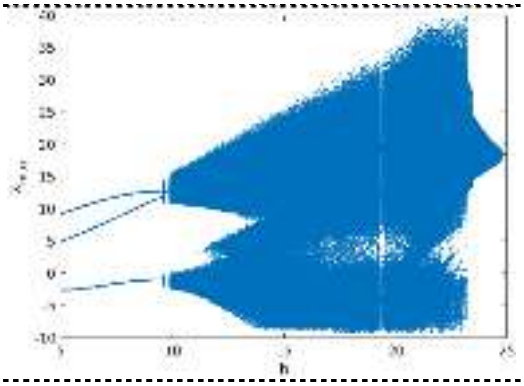

Figure 8. Bifurcation transition plot of $x_{\max}$ as b increases the 4-D system (10)

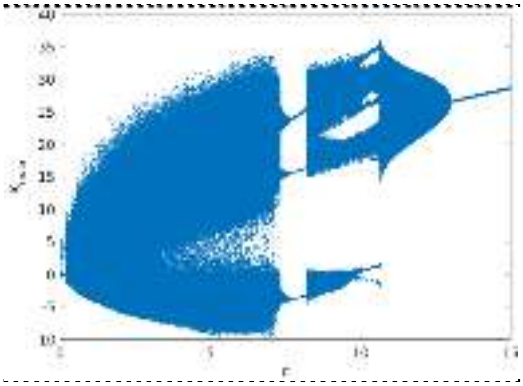

Figure 9. Bifurcation transition plot of $x_{\max}$ as c decreases the 4-D system (10)

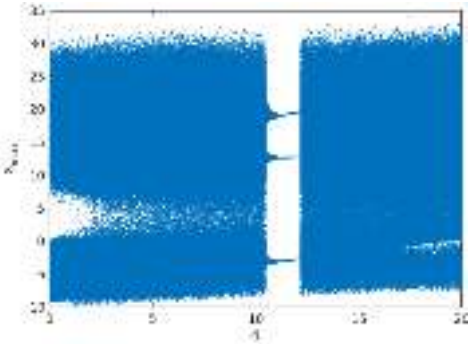

Figure 10. Bifurcation transition plot of $x_{\max}$ as d increases the 4-D system (10)

4. Circuit Implementation of the New Hyperchaotic System

This study will consider the analog circuit implementation of the new hyperchaotic two-wing system described in (1). Figure 11 shows a four channels electronic circuit scheme with variables x, y, z, w from the system (1). The analog circuit of the new hyperchaotic system is realized by resistors, capacitors, operational amplifiers and multipliers. By applying Kirchhoff's laws to this circuit, its dynamics are presented by the following circuital equations:

$$\begin{cases} \dot{x} = \dfrac{1}{C_1 R_1} y - \dfrac{1}{C_1 R_2} x + \dfrac{1}{10 C_1 R_3} yz + \dfrac{1}{C_1 R_4} w \\ \dot{y} = \dfrac{1}{C_2 R_5} y - \dfrac{1}{10 C_2 R_6} xz + \dfrac{1}{C_2 R_7} w \\ \dot{z} = -\dfrac{1}{C_3 R_8} z + \dfrac{1}{10 C_3 R_9} xy \\ \dot{w} = -\dfrac{1}{C_4 R_{10}} x \end{cases} \tag{14}$$

Where x, y, z, w are the voltages across the capacitors C_1, C_2, C_3 and C_4, respectively. the values of the circuit elements can be determined: $R_1 = R_2 = 12.12$ kΩ, $R_3 = R_6 = R_9 = 40$ kΩ, $R_4 = R_7 = 400$ kΩ, $R_5 = 22.22$ kΩ, $R_8 = 80$ kΩ, $R_{10} = R_{11} = R_{12} = R_{13} = R_{14} = R_{15} = R_{16} = 100$ kΩ, $C_1 = C_2 = C_3 = C_4 = 3.2$ nF. After validation using MultiSIM, we can see a two-wing chaotic attractor from the oscilloscope as shown in Figures 12-15. Obviously, the MultiSIM results same with the theoretical model system (1).

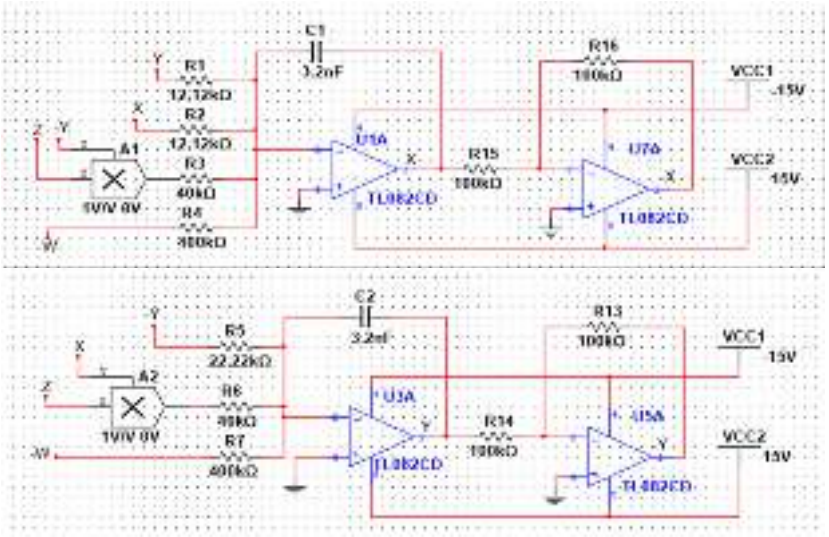

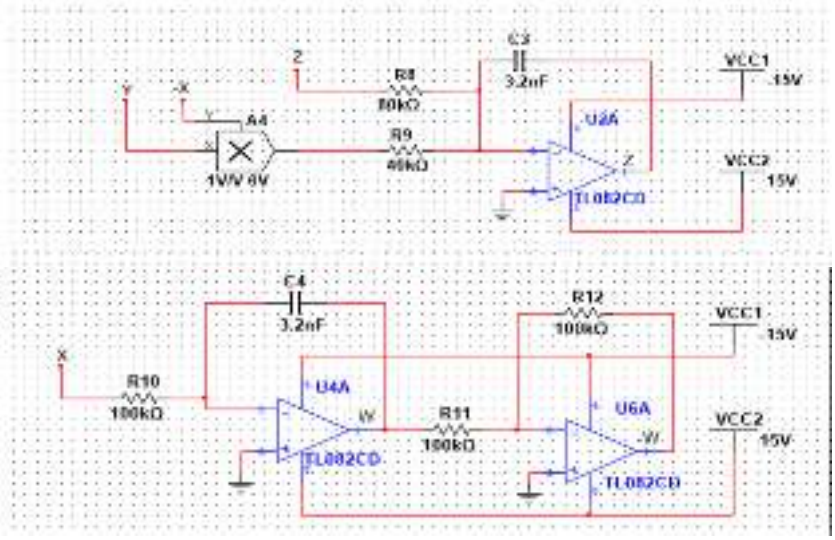

Figure 11. Circuit design for the new hyperchaotic system (1)

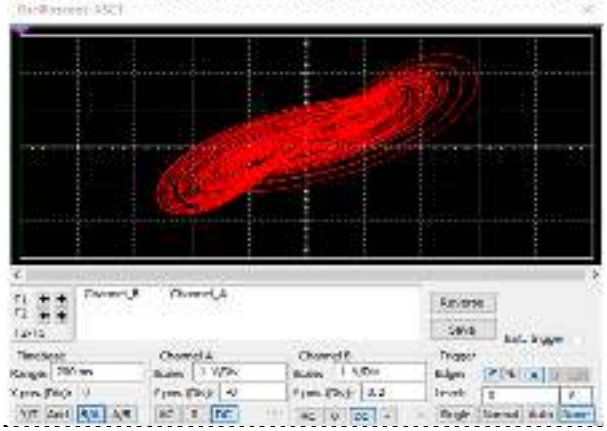

Figure 12. MultiSIM output of the new hyperchaotic system in $(x, y)-$plane

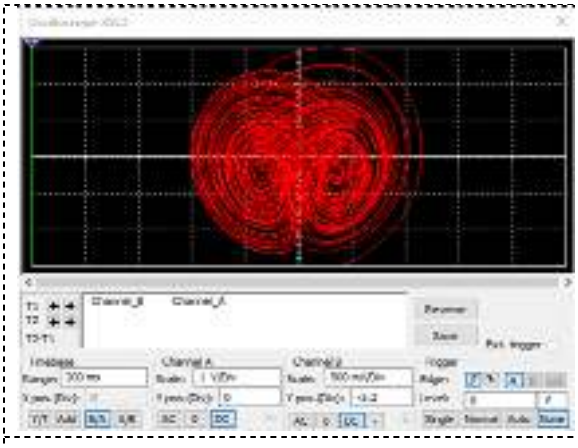

Figure 13. MultiSIM output of the new hyperchaotic system in $(y, z)-$plane

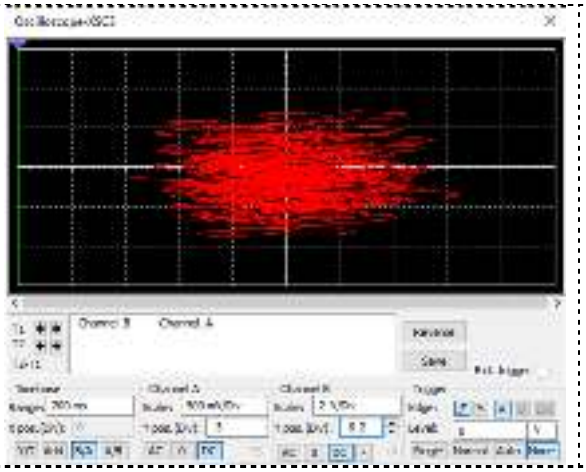

Figure 14. MultiSIM output of the new hyperchaotic system in $(z, w)-$plane

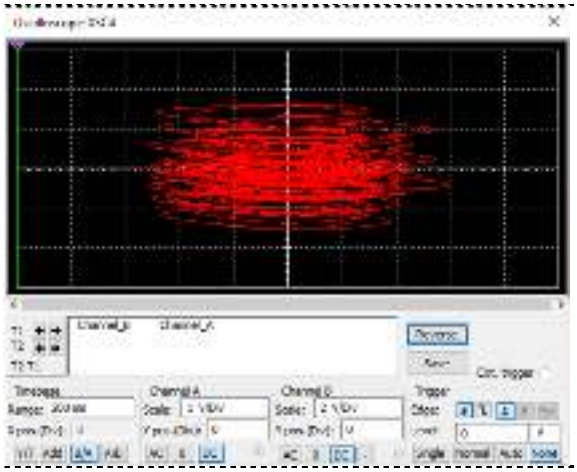

Figure 15. MultiSIM output of the new hyperchaotic system in $(x, w)-$plane

5. Conclusions

A new 4-D hyperchaotic two-wing system with three quadratic nonlinearities is proposed in this paper. The dynamical properties of the new hyperchaotic system were analyzed with the help of phase portraits, Lyapunov exponents, Kaplan-Yorke dimension, bifurcation diagrams, symmetry, dissipativity, etc. As an engineering application, an electronic circuit realization of the new hyperchaotic two-wing system was developed in MultiSIM. We demonstrated that the MultiSim outputs of the new hyperchaotic two-wing system show good agreement with the MATLAB simulations of the system. Thus, the proposed new hyperchaotic two-wing system can be implemented for many real-world applications.

References

[1] Vaidyanathan S and Volos C 2017 *Advances and Applications in Chaotic Systems* (Berlin: Springer)
[2] Pham V T, Vaidyanathan S, Volos C and Kapitaniak T 2018 *Nonlinear Dynamical Systems with Self-Excited and Hidden Attractors* (Berin: Springer)
[3] Vaidyanathan S, Azar A T, Rajagopal K, Sambas A, Kacar S and Cavusoglu U 2018 *International Journal of Simulation and Process Modelling* **13** 281-296
[4] Vaidyanathan S, Volos C K, Rajagopal K, Kyprianidis I M and Stouboulos I N 2015 *Journal of Engineering Science and Technology Review* **8** 74-82
[5] Rasappan S and Vaidyanathan S 2012 *Far East Journal of Mathematical Sciences* **67** 265-287
[6] Vaidyanathan S 2015 *International Journal of PharmTech Research* **8** 622-631
[7] Vaidyanathan S 2015 *International Journal of PharmTech Research* **8** 974-981
[8] Vandermeer J and Perfecto I 2017 *Agroecology and Sustainable Food Systems* **41** 697-722
[9] Pal N, Samanta S and Rana S 2017 *International Journal of Applied and Computational Mathematics* **3** 3615-3644
[10] Chang L and Jin Z 2018 *Applied Mathematics and Computation* **316** 138-154
[11] Vaidyanathan S 2015 *International Journal of PharmTech Research* **8** 167-177
[12] Vaidyanathan S 2015 *International Journal of PharmTech Research* **8** 956-963
[13] Tomita K 1982 *Journal of Theoretical Biology* **99** 111-118
[14] Vaidyanathan S 2015 *International Journal of PharmTech Research* **8** 106-116
[15] Vaidyanathan S 2015 *International Journal of PharmTech Research* **8** 156-166
[16] Din Q, Shabbir M S, Khan M A and Ahmad K 2019 *Journal of Biological Dynamics* **13** 481-501
[17] Njitacke Z T and Kengne J 2018 *AEU-International J. Electronics and Communications* **93** 242-252
[18] Vaidyanathan S 2015 *International Journal of PharmTech Research* **8** 946-955
[19] Saad M, Safieddine A and Sultan R 2018 *Journal of Physical Chemistry A* **122** 6043-6047
[20] Vaidyanathan S 2015 *International Journal of ChemTech Research* **8** 159-171
[21] Vaidyanathan S 2015 *International Journal of ChemTech Research* **8** 740-749
[22] Vaidyanathan S 2015 *International Journal of ChemTech Research* **8** 146-158
[23] Vaidyanathan S 2015 *International Journal of ChemTech Research* **8** 669-683
[24] Vaidyanathan S 2015 *International Journal of ChemTech Research* **8** 209-221
[25] Faust O, Acharya U R, Adeli H and Adeli A 2015 *Seizure* **26** 56-64
[26] Vaidyanathan S 2015 *International Journal of PharmTech Research* **8** 964-973
[27] Vaidyanathan S 2015 *International Journal of ChemTech Research* **8** 818-827
[28] Maggs J E, Rhodes T L and Morales G J 2015 *Plasma Physics and Controlled Fusion* **57** 045004
[29] Hellen E H and Volkov E 2018 *Communications in Nonlinear Science and Numerical Simulation* **62** 462-479
[30] Vaidyanathan S 2013 *Lecture Notes in Electrical Engineering* **131** 319-327
[31] Vaidyanathan S 2015 *International Journal of Modelling, Identification and Control* **23** 380-

392
[32] Vaidyanathan S and Rajagopal K 2011 *Communications in Computer and Information Science* **205** 193-202
[33] Vaidyanathan S 2012 *Lecture Notes of the Institute for for Computer Sciences, Social-Informatics and Telecommunications Engineering* **85** 124-133
[34] Vaidyanathan S, Volos C and Pham V T 2015 *Studies in Computational Intelligence* **576** 571-590
[35] Pham V T, Vaidyanathan S, Volos C K, Jafari S, Kuznetsov N V and Hoang T M 2016 *European Physical Journal: Special Topics* **225** 127-136
[36] Xu Q, Zhang Q, Jiang T, Bao B and Chen M 2018 *Circuit World* **44** 108-114
[37] Vaidyanathan S, Sambas A, Mamat M and Sanjaya W S M 2017 *Archives of Control Sciences* **27** 541-554
[38] Singh J P, Lochan K, Kuznetsov N V and Roy B K 2017 *Nonlinear Dynamics* **90** 1277-1299
[39] Wang Y, Mou Y and Zhang J 2018 *Journal of Harbin Engineering University* **39** 584-593
[40] Mansour S M B, Sundarapandian V and Naceur S M 2016 *International Journal of Control Theory and Applications* **9** 37-54
[41] Vaidyanathan S and Rajagopal K 2017 *International Journal of Simulation and Process Modelling* **12** 165-178
[42] Dou Y, Liu X, Fan H and Li M 2017 *Optik* **145** 456-464
[43] Vaidyanathan S, Sambas A, Mamat M and Sanjaya W S M 2017 *International Journal of Modelling, Identification and Control* **28** 153-166
[44] Idowu B A, Vaidyanathan S, Sambas A, Olusola O I and Onma O S 2018 *Studies in Systems, Decision and Control* **133** 271-295
[45] Tacha O I, Volos C K, Kyprianidis I M, Stouboulos I N, Vaidyanathan S and Pham V T 2016 *Applied Mathematics and Computation* **276** 200-217
[46] Volos C K, Pham V T, Vaidyanathan S, Kyprianidis I M and Stouboulos I N 2015 *Journal of Engineering Science and Technology Review* **8** 142-151
[47] Daltzis P, Vaidyanathan S, Pham V T, Volos C, Nistazakis E. and Tombras G. 2018 *Circuits, Systems, and Signal Processing* **37** 613-615
[48] Sambas A, Vaidyanathan S, Mamat M and Mada Sanjaya W S 2018 *Studies in Systems, Decision and Control* **133** 365-373
[49] Pham V T, Jafari S, Volos C, Giakoumis A, Vaidyanathan S and Kapitaniak T 2016 *IEEE Transactions on Circuits and Systems II: Express Briefs* **63** 878-882
[50] Sambas A, Vaidyanathan S, Zhang S, Zeng Y, Mohamed M A and Mamat M 2019 *IEEE Access* **7** 115454-115462
[51] Arabyani H and Nik H S 2016 International Journal of Modelling, Identification and Control 25 138-144
[52] Ouannas A, Grassi G, Ziar T and Odibat Z 2017 *Optik* **136** 513-523
[53] Mahmoud G M, Mahmoud E E and Arafa A A 2015 *Nonlinear Dynamics* **80** 855-869
[54] Vaidyanathan S, Dolvis L G, Jacques K, Lien C H and Sambas A 2019 *International Journal of Modelling, Identification and Control* **32** 30-45
[55] Vaidyanathan S, Azar A T and Boulkroune A 2018 *International Journal of Automation and Control* **12** 5-26
[56] Wolf A, Swift J B, Swinney H L and Vastano J A 1985 *Physica D* **16** 285-317